

A technique for estimation of starburst masses and ages in luminous compact galaxies

S. L. Parnovsky • I. Y. Izotova

© Springer-Verlag 0000

Abstract We propose a technique for estimation of the mass m of the young stellar population and the starburst age T in luminous compact galaxies (LCGs). For this purpose we use LCG H α emission line luminosities from the Sloan Digital Sky Survey (SDSS) spectra and *Galaxy Evolution Explorer (GALEX)* FUV and NUV continuum luminosities. The method is intended for quick estimation of m and T in large galaxy samples and does not require spectral energy distribution (SED) fitting. Estimated m and T for the sample of about 550 LCGs are compared with the same values derived from the SED fitting in the wavelength range $\lambda\lambda 3800 - 9200\text{\AA}$. We obtain the average differences in $\log m$ and T of 0.27 and 0.87 Myr, respectively. This technique could be used for selection of galaxies with desired ranges of m and T or for reducing a range of parameter variations in SED fitting.

Keywords Galaxies: starburst — Galaxies: star formation — Galaxies

1 Introduction

The goal of this article is to describe a method for estimating some starburst parameters of luminous compact galaxies (LCGs). LCGs are characterised by a strong

burst of star formation (Izotov et al. 2011) and have the properties similar to those in so called “green pea” (GP) galaxies discussed by Cardamone et al. (2009).

GPs were selected from the Sloan Digital Sky Survey (SDSS) images (Abazajian et al. 2009) in the framework of the Galaxy Zoo project as compact objects with a green color. This color indicates the presence of strong [O III] $\lambda 5007$ emission line redshifted to the SDSS r band in galaxies with redshifts $z \sim 0.1 - 0.3$.

On the other hand, LCGs were selected from the SDSS spectra as the objects with strong emission lines and they are characterised by a wider range of redshifts $z \sim 0.02 - 0.6$ (Izotov et al. 2011). Therefore, depending on the redshift, LCGs on composite SDSS images can be blue, pink, white, green, brown while other characteristics are the same as those in GPs. Selection criteria and derived global characteristics of LCGs are described in Izotov et al. (2011). Briefly, these criteria were as follows: high equivalent width and large luminosity of the H β emission line ($\text{EW}(\text{H}\beta) \geq 50\text{\AA}$, $L(\text{H}\beta) \geq 3 \times 10^{40} \text{ erg s}^{-1}$, respectively); well-detected [O III] $\lambda 4363\text{\AA}$ emission line in galaxy spectra, with a flux error less than 50%. Only star-forming galaxies with typical angular diameters $\leq 10''$ were selected. All these criteria only select objects with strong emission lines in their spectra and thus with young starburst ages 3 - 5 Myr for which the accurate abundance determination using the direct method is possible. Izotov et al. (2011) concluded that GPs sample is a subset of a larger sample of ~ 800 LCGs in a relatively narrow range of redshifts.

General properties of GPs and LCGs seem to be uncommon in the nearby universe suggesting a short and extreme phase of their evolution (Amorín et al. 2010) and may represent the star formation mode prevailing in the early Universe (Cardamone et al. 2009). LCGs and GPs are characterised by low oxygen abundance (of $\sim 20\%$ solar) (Amorín et al. 2010; Izotov et al. 2011;

S. L. Parnovsky

Astronomical Observatory of Taras Shevchenko Kyiv National University
 Observatorna str., 3, 04053, Kyiv, Ukraine
 tel: +380444860021, fax: +380444862191
 e-mail:par@observ.univ.kiev.ua

I. Y. Izotova

Astronomical Observatory of Taras Shevchenko Kyiv National University
 Observatorna str., 3, 04053, Kyiv, Ukraine
 tel: +380444860021, fax: +380444862191
 e-mail:izotova@observ.univ.kiev.ua

Pilyugin et al. 2012; Hawley 2012), low stellar mass of $\sim 10^{8.5} - 10^{10} M_{\odot}$, high star formation rates (SFR $\sim 10 M_{\odot} \text{yr}^{-1}$) and high specific star formation rate (up to $\sim 10^{-8} \text{yr}^{-1}$) (Cardamone et al. 2009; Izotov et al. 2011). These features place LCGs and GPs between nearby blue compact dwarf (BCD) galaxies on one side and high-redshift UV-luminous Lyman-break galaxies (LBG) and Ly α emitters on the other side.

Parnovsky et al. (2013) used the regression analysis to study the dependence of the LCG monochromatic luminosities in the *Galaxy Evolution Explorer (GALEX)* far-UV (FUV, $\lambda_{\text{eff}} = 1528 \text{\AA}$) and near-UV (NUV, $\lambda_{\text{eff}} = 2271 \text{\AA}$) bands and the H α emission line luminosities on parameters derived by Izotov et al. (2011) for LCGs. Izotov et al. (2011) used all LCG spectra and Monte Carlo simulations to fit spectral energy distributions (SED) in the wavelength range $\lambda\lambda 3800 - 9200 \text{\AA}$. As far as the spectral contribution of the gaseous continuum in LCGs is high, it was fitted first using equivalent width EW(H β) of the H β emission line and subtracted from the observed spectrum prior to the fitting of the stellar continuum. It is assumed that young stars were formed in a single burst with the age which is varied in the range 0 – 10 Myr. It is also adopted that old stars were formed continuously with a constant star formation rate. The fitting provided the set of parameters for each galaxy, namely the masses of young m and old $M(\text{old})$ stellar populations, the age of a starburst T , and the lower (t_2) and upper (t_1) limits for the age of old stars (see more details in Izotov et al. 2011). Parnovsky et al. (2013) found that only three parameters, namely oxygen abundance 12+logO/H, the mass m and the age T of the young stellar population have the statistically significant impact on the luminosity. More specifically, LCG luminosities $L(\text{FUV})$, $L(\text{NUV})$ and $L(\text{H}\alpha)$ are proportional to the mass m while the ratio L/m depends on the age of the starburst T . Thus these parameters are fundamental to study the evolution of LCG luminosity.

In the present paper we propose a simple technique for estimating of the young stellar population mass m and age T from the LCGs luminosities in three wavelength bands without invoking SED fitting. We give a brief description of the method in Section 2 and provide details in Section 3. In Section 4 we describe one of the variants of the proposed method. In Section 5 we describe the sample and its subsamples considered in this paper. The parameters, which are necessary for m and T estimation, are discussed in Section 6. In Section 7 we compare the values m and T derived with technique proposed in this paper to those obtained by Izotov et al. (2011) from fitting the SED of galaxies, and estimate the accuracy of the proposed method. In

Section 8 we consider the accuracy of the method excluding the oxygen abundances [O] from the parameter set. The accuracy of the m and T estimation from luminosities only at two wavelengths is discussed in Section 9. In Section 10 we summarise the main results of this paper.

For distance estimates we assume $H_0 = 75 \text{ km s}^{-1} \text{Mpc}^{-1}$.

2 Description of the method

We describe the method using the results of the paper by Parnovsky et al. (2013). To simplify the way of comparing $L(\text{H}\alpha)$, $L(\text{FUV})$ and $L(\text{NUV})$, Parnovsky et al. (2013) used the calibration for SFRs averaged over a reasonable time scale for different SFR tracers and defined by Kennicutt (1998) as

$$\text{SFR} = k \times L. \quad (1)$$

The conversion factors k between the SFR and $L(\text{H}\alpha)$, $L(\text{FUV})$ and $L(\text{NUV})$ as well as other star formation tracers are discussed by Calzetti (2012). Kennicutt (1998) derived the coefficient k of 7.9×10^{-42} for the H α luminosity and 1.4×10^{-28} for the FUV and NUV luminosities assuming the solar metallicity, the initial mass function with the power-law index 2.35 and mass limits of 0.1 and $100 M_{\odot}$ (Salpeter 1955), and expressing SFR in $M_{\odot} \text{ yr}^{-1}$, $L(\text{H}\alpha)$ in erg s^{-1} , $L(\text{FUV})$ and $L(\text{NUV})$ in $\text{erg s}^{-1} \text{ Hz}^{-1}$. We use these coefficients to calculate SFR values for the sample of LCGs.

According to Parnovsky et al. (2013) the statistical dependence of the luminosity of an individual galaxy on its parameters has the form

$$\text{SFR} = m (Af(t) + B\Delta) \quad (2)$$

with

$$f(t) = \begin{cases} 1 & \text{if } t < 0; \\ \exp(-pt) & \text{if } t > 0, \end{cases} \quad (3)$$

where $t = T - T_0$, $\Delta = [\text{O}] - [\text{O}]_0$, $[\text{O}] \equiv 12 + \log(\text{O/H})$ is the oxygen abundance, and A , B and p are constants. We also use two parameters $T_0 = 3.2 \text{ Myr}$ and $[\text{O}]_0 = 8.1$. Parnovsky et al. (2013) chosen the parameter $[\text{O}]_0$ as the mean oxygen abundance either of the entire sample or its subsamples. In the present paper few subsamples are considered, therefore we fix the value $[\text{O}]_0 = 8.1$ which is the mean oxygen abundance of the entire sample. According to Eq. 3, the SFR and the luminosity of the galaxy are constant for $T < T_0$ and decrease exponentially for $T > T_0$. This dependence on time is applicable to H α , FUV and NUV luminosities

with the same value $T_0 = 3.2$ Myr corresponding to the lifetime of the most massive stars with a mass $\sim 100 M_\odot$. The similar dependence in Eq. 2 and the same value of T_0 for strongly star-forming LCGs revealed by Parnovsky et al. (2013) imply that $\text{H}\alpha$, FUV and NUV emissions in LCGs are produced by the same young stellar populations. These facts justify the applicability of the m and T estimation from the luminosities in different bands.

The ionising radiation responsible for $\text{H}\alpha$ emission is produced by the most massive O stars, while B stars with longer lifetimes contribute to the FUV and NUV bands, in addition to O stars. Therefore, the FUV and NUV luminosities decrease with time more slowly compared to the $\text{H}\alpha$ luminosity, satisfying inequalities $p(\text{H}\alpha) > p(\text{FUV}) > p(\text{NUV})$.

Combining equations (1) and (2) we obtain relations

$$L = m (A^* f(t) + B^* \Delta), \quad A^* = A \times k, \quad B^* = B \times k. \quad (4)$$

Thus, only two parameters A^* and B^* for the determination of m and T are needed. We note that it is not necessary to know the correct values of k for $\text{H}\alpha$ line and UV radiation. Overrating the real value k_{real} by a factor w and using the value $k = w \times k_{\text{real}}$, we obtain $A = w^{-1} \times A_{\text{real}}$ and $B = w^{-1} \times B_{\text{real}}$ instead of correct values A_{real} and B_{real} . However, A^* and B^* remain unchanged and overrating does not affect the m and T values.

For comparison of LCG SFRs with SFRs derived in different studies for galaxies of different types we adopt the coefficient k in Eq. 1 proposed by Kennicutt (1998) for continuous or quasi-continuous star formation which is common in big galaxies with frequent starbursts. This value of k may not be used for LCGs where star formation occurs in strong and rare bursts. However, the variations of k do not influence the m and T values, as discussed above.

The dependence in Eq. 2 for emission in the $\text{H}\alpha$ line, FUV or NUV continuum is characterised by only three parameters A , B and p . We introduce the index $i = 1, 2, 3$ denoting the $\text{H}\alpha$, FUV and NUV spectral bands, respectively. Luminosity decay times for $\text{H}\alpha$ line and in the FUV or NUV ranges are given by $\tau_i = p_i^{-1}$. The relations $p_1 > p_2 > p_3$ and respectively $\tau_1 < \tau_2 < \tau_3$ are satisfied for our LCG subsamples (see Table 1). The ratios of $L(\text{H}\alpha)$ to $L(\text{FUV})$ or $L(\text{NUV})$ and $L(\text{FUV})$ to $L(\text{NUV})$ decrease exponentially at $T > T_0$. Therefore, one can determine the value of T using any of these ratios.

The details of this procedure are described in Section 9. To apply the proposed method one has to know the set of parameters A_i , B_i and p_i for the FUV or NUV bands and/or the $\text{H}\alpha$ line. In Section 6 we describe how

to obtain these parameters. Each set of parameters for the $\text{H}\alpha$ line and the FUV and NUV range is the common one for the entire LCG sample. To estimate m and T for individual galaxy one has also to know its luminosities in the FUV or NUV bands and/or in the $\text{H}\alpha$ line, as well as its oxygen abundance $[\text{O}]$.

One cannot determine the starburst age T if $T < T_0$, where luminosities and their ratios do not depend on the time. However, we can identify such a situation and this information is sufficient for the determination of the initial luminosities L_0 at the starburst age $T = 0$ introduced by Parnovsky et al. (2013). The initial $\text{H}\alpha$, FUV and NUV luminosities can be obtained from current luminosities and the value $f(T)$ from Eq. 2. If we know the value of $T > T_0$ or the fact that $T < T_0$, the value of m can be derived from the $\text{H}\alpha$, FUV and NUV luminosities using Eq. 2.

The estimation of m and T from the luminosities only in two wavelength bands is not very accurate due to the influence of measurement errors and deviations from the statistical relation in Eq. 2. On the other hand, the estimation of m and T values from the luminosities in all three wavelength bands is more accurate. It is described in Section 3.

3 The estimation of m and T values from the luminosities at three wavelengths

Using Eq. 2 one can determine m and T for each galaxy minimizing the expression

$$U = \sum_{i=1}^3 \left(\frac{SFR_i - m(A_i f_i(t) + B_i \Delta)}{\sigma_i} \right)^2. \quad (5)$$

where U is the sum of the weighted deviations of $\text{H}\alpha$, FUV and NUV luminosities. Here we use different statistical weights for data at different wavelengths. They are chosen inversely proportional to the variances σ_i^2 , where σ_i are mean dispersion for the approximation in Eq. 2 at each of three wavelengths. These values are also obtained in Section 6.

The derivative of U with respect to m should be equal to zero. This requirement yields the condition

$$m = \frac{\sum_{i=1}^3 SFR_i (A_i f_i + B_i \Delta) \sigma_i^{-2}}{\sum_{i=1}^3 (A_i f_i + B_i \Delta)^2 \sigma_i^{-2}}. \quad (6)$$

If $t = T - T_0 > 0$, we have $df_i(t)/dT = -f_i p_i$ from Eq. 3 and the condition $\partial U / \partial T = 0$ has the form

$$\sum_{i=1}^3 SFR_i A_i f_i p_i \sigma_i^{-2} = m \sum_{i=1}^3 (A_i f_i + B_i \Delta) A_i f_i p_i \sigma_i^{-2}.$$

(7)

If $t > 0$, the numerical solution of Eq. 7 together with Eq. 6 and $f_i = \exp(-p_i t)$ provides an estimated value of t . Then we derive $T_e = T_0 + t$ while Eq. 6 provides an estimation of m . In the case of $t < 0$ ($T_e \leq T_0$) we derive the estimation of m from Eq. 6 adopting $f_i = 1$. In such a way we obtain the estimations of the age T of the starburst, which we denote T_e , and the mass m of the young stellar population, which we denote m_e (subscript e means estimated).

4 Alternative version of the method of m and T determination

Consider an alternative version of the method which slightly differs from the one mentioned in Section 3. From Eq. 2 we obtain

$$\frac{SFR}{m} = \tilde{A}\tilde{f}(t) + \tilde{B}\Delta, \quad (8)$$

The values of \tilde{A}_i and \tilde{B}_i are obtained by the least squares method using the approximation in Eq. 8. They slightly differ from the values A_i and B_i used in Section 3. Then m and T are derived from minimization of the expression

$$\tilde{U} = \sum_{i=1}^3 \left(\frac{SFR_i/m - \tilde{A}_i \tilde{f}_i(t) - \tilde{B}_i \Delta}{\tilde{\sigma}_i} \right)^2. \quad (9)$$

Here $\tilde{\sigma}_i$ are mean dispersions of the data around the approximation in Eq. 8 at three wavelengths. The condition $\partial\tilde{U}/\partial T = 0$ corresponds to Eq. 7, but with tildes above the A , B , f and p . The condition $\partial\tilde{U}/\partial m = 0$ yields

$$m = \frac{\sum_{i=1}^3 SFR_i^2 \tilde{\sigma}_i^{-2}}{\sum_{i=1}^3 SFR_i (\tilde{A}_i \tilde{f}_i + \tilde{B}_i \Delta) \tilde{\sigma}_i^{-2}}. \quad (10)$$

instead of Eq. 6. If the numerical solution of Eq. 7 with Eq. 10 and $\tilde{f}_i = \exp(-\tilde{p}_i t)$ corresponds to $t > 0$, we have the estimation $\tilde{T}_e = T_0 + t$ with the different value of t as compared to the one in Section 3. In the case $t < 0$ we derive the estimation $\tilde{T}_e \leq T_0$ while Eq. 10 with $\tilde{f}_i = 1$ provides the value of \tilde{m}_e . As a result we obtain somewhat different estimations of the ages of the starburst and the masses of the young stellar population for LCGs. We denote the estimation obtained by the prior method as m_e and T_e and the estimation derived by the latter method as \tilde{m}_e and \tilde{T}_e .

It is not known a priori which of these methods is better, but the detailed analysis carried out in Section

7 shows that the alternative version of the method provides much worse estimation than the first one. This follows from the comparison of the values obtained by both methods and the values m_f and T_f derived from SED fitting. Hereafter the subscript f means “fitted” and refers to the values obtained by Izotov et al. (2011).

5 Sample and subsamples

For the determination of the starburst age T and the mass m of the young stellar population in the individual galaxy we need SFR_i derived from the $H\alpha$, FUV, and NUV luminosities and Δ derived from the oxygen abundance $[O]$. We use the calibration sample of about 800 LCGs constructed by Izotov et al. (2011). The FUV and NUV fluxes for LCGs were extracted from the GALEX Medium Imaging Survey (MIS) and All-sky Imaging Survey (AIS) data. These data combined with the SDSS data on $H\alpha$ fluxes and redshifts (Izotov et al. 2011) provide the determination of the galaxies $H\alpha$ and UV luminosities.

Because the radiation of galaxies is reduced by dust extinction, we applied reddening corrections to $H\alpha$ and UV band fluxes using Cardelli et al. (1989) reddening law. All $H\alpha$ emission line luminosities are also corrected for aperture (see details in Parnovsky et al. 2013).

In Parnovsky et al. (2013) the sample of LCGs was splitted into two subsamples of “regular” galaxies with the round shape and “irregular” galaxies with some sign of disturbed morphology suggesting the presence of two or more star-forming regions and their interaction. To clarify the impact of the LCG’s morphology on the obtained parameters we instead of these two subsamples produce seven subsamples on the base of detailed visual examination of galaxies morphology on SDSS images. We marked the galaxies with 2-3 evident knots of star formation separated by $\leq 10''$ in the subsample of “irregular” galaxies. In addition we marked galaxies with a single star-forming region, but with an obvious visual asymmetry, e.g. in the form of some small “tail” or a sign of a “tail”. Summarising, we split the LCG sample on the following subsamples. I – “regular” galaxies. II – “irregular” galaxies. These subsamples are practically the same as the subsamples used by papers Izotov et al. (2011) and Parnovsky et al. (2013). III – “irregular” galaxies with a single star-forming region. It is formed from the subsample II after discarding of galaxies with two or three possible star-forming regions. IV – “irregular” galaxies with a single star-forming region without obvious visual asymmetry. IV is a subset of III and III is a subset of II. Combining I with II, III or IV we produce three more subsamples. V is a combination of subsamples I and II, this is the entire initial

sample. VI is a combination of subsamples I and III, it contains all the galaxies with a single star-forming region. VII is a combination of subsamples I and IV, it contains all galaxies with a single star-forming region without obvious asymmetry.

These subsamples can be additionally constrained according to the errors in the measured UV fluxes. Our initial entire LCG sample includes only galaxies with the UV flux errors not exceeding 50%, but we can also impose a more strict limitation on the errors. The flux error limitation in the first column of Table 1 is shown as the percentage of the UV flux. The word “all” means the initial 50% error level, designations 30%, 20% and 10% indicate the reduced thresholds of UV flux errors. Note that these thresholds apply to the fluxes both in FUV and NUV ranges.

6 Determination of parameters A , B , p and σ

Three sets of parameters A_i, B_i, p_i, σ_i in approximations Eq. 2 are needed to estimate m and T . The determination of these parameters is described in details by Parnovsky et al. (2013). It was carried out by the least squares method and the linear regression analysis.

We use the least squares method to calculate the sets of parameters in Eq. 2 for all subsamples described in Section 5. The number N of the galaxies, the values of p_i in Myr^{-1} , σ_i in $M_\odot \text{ yr}^{-1}$, A_i and B_i in yr^{-1} are shown in Table 1.

The parameters in Parnovsky et al. (2013) are almost the same as the ones in the first row (label “all” in the first column) in the part of Table 1 corresponding to the subsample V. It differs from the sample used in Parnovsky et al. (2013) only by excluding one obvious outlier from the subsample of “regular” galaxies.

One can see from Table 1 that discarding galaxies with possible several star-forming regions and asymmetry noticeably decreases the variance, as well as the flux errors limitation. This effect becomes stronger if the galaxies with the pronounced asymmetry are also excluded. The F-test (Fisher 1954; Hudson 1964) shows that the statistical significance of the first term on the right side of Eq. 2 is very high and the statistical significance of the second term exceeds 99% level for the majority of subsamples. It becomes statistically insignificant only for FUV radiation and subsamples IV and VII with flux errors less than 10%.

The values of σ_1 are less than σ_2 and σ_3 due to a better accuracy of $\text{H}\alpha$ flux measurements. The values of σ_2 and σ_3 for the samples with flux errors limitation are decreased with increasing of flux accuracy. The

difference between A_i values indicates that the k factors have to be corrected for better agreement between SFRs derived from fluxes at different wavelengths. Corresponding changes were proposed and the ratios of new k values for FUV, NUV and $\text{H}\alpha$ were found in (Parnovsky et al. 2013). In the present paper we dont compare the SFRs derived using different tracers. We use the equal k values for FUV and NUV ranges and use the k value for $\text{H}\alpha$ line estimated for the galaxies with different properties (Kennicutt 1998). This do not affect the accuracy of m and T estimation but leads to the difference between the values of A_i for different tracers.

The values of the coefficients A_i, B_i and p_i , derived from different subsamples, vary insignificantly. Nevertheless, small variations of these coefficients result in a noticeable change of data scatter and σ_i . Thus, it is important to use a set of the coefficients calculated for a properly refined subsample.

We choose the values for the subsample VII with UV flux errors smaller than 20% as the set of coefficients for Eq. 2. For each galaxy we estimate T_e and m_e using the coefficients $\sigma_i = (3.0, 4.2, 4.7)$, $p_i = (0.72, 0.35, 0.27)$, $A_i = (2.06 \times 10^{-7}, 1.04 \times 10^{-7}, 1.43 \times 10^{-7})$ and $B_i = (-4.72 \times 10^{-8}, -6.21 \times 10^{-8}, -9.21 \times 10^{-8})$.

The parameters \tilde{p}_i , \tilde{A}_i , \tilde{B}_i and $\tilde{\sigma}_i$ in Eq. 8 for the subsamples shown in Table 1 were calculated by the least squares method as well. Note that this approximation is the same as given by Eq. 2, but with statistical weights proportional to m^{-2} , which makes it more sensitive to the data for small galaxies. The values of \tilde{p} in this case are larger than those for the approximation Eq. 2 and closer to each other. We choose the values for the subsample VII with UV flux errors smaller than 30% as the sets of coefficients for Eq. 8. We estimate \tilde{T}_e and \tilde{m}_e using the coefficients $\tilde{\sigma}_i = (6.0 \times 10^{-8}, 6.1 \times 10^{-8}, 8.1 \times 10^{-8}) \text{ yr}^{-1}$, $\tilde{p}_i = (0.70, 0.51, 0.50)$, $\tilde{A}_i = (2.20 \times 10^{-7}, 1.26 \times 10^{-7}, 1.65 \times 10^{-7})$ and $\tilde{B}_i = (-6.90 \times 10^{-8}, -9.72 \times 10^{-8}, -8.93 \times 10^{-8})$. The parameters for other subsamples are close to these values.

7 On the method accuracy

Compare the values m_e and T_e obtained by the method proposed in Section 3 and based on Eqs. 6-7 with the values m_f and T_f obtained in Izotov et al. (2011) by fitting the galaxy SEDs. Although we can estimate m_e and T_e for almost every galaxy from the sample, using the entire sample is a poor choice for such a comparison due to the presence of galaxies with several star-forming regions for which the values of m_e and T_e can differ substantially. The described method is intended for quick

estimation of the values m_e and T_e in large LCCs samples without SED fitting. Note that such samples may contain both “regular” and “irregular” galaxies. We can exclude galaxies with several star-forming regions and, if desired, galaxies with an asymmetry by visual inspection of SDSS images. Thus we use the subsamples VI or VII for more reliable and accurate comparison. In addition we can constrain the values of UV flux errors.

In Fig. 1 we show an example for the subsample VI. Dots correspond to “regular” galaxies from subsample I, open circles – to “irregular” galaxies with a single star-forming region without obvious asymmetry from subsample IV, and triangles – to “irregular” galaxies with a single star-forming region with obvious asymmetry. Triangles together with open circles correspond to subsample III. It is seen that the estimated m roughly match the masses obtained from SED fitting. The largest deviations occur for asymmetric LCCs.

We estimate the accuracy of the proposed method. Note that three values SFR_i are used to derive two values m_e and T_e . Thus, we still have a possibility to obtain one additional parameter for each LCG which is a characteristic of the consistency between different m estimates. Given the value of T_e derived from Eqs. 6-7 we can obtain three different estimations of m_e using only galaxy luminosities at three wavelengths as

$$m_i = \frac{SFR_i}{A_i f_i + B_i \Delta} \quad (11)$$

The estimations in Eqs. 6 or 10 are weighted averages of these values.

We choose the root-mean-square value of the logarithm of the m_e to m_f ratio as the indicator of deviations and define the quantity

$$q = \left(\frac{\sum_{k=1}^N \log^2(m_e/m_f)_k}{N} \right)^{1/2}. \quad (12)$$

In Table 2 we present the values of q for different subsamples.

One can see from Table 2 that the values of q are substantially larger for the II and V subsamples containing galaxies with several star-forming regions as compared to the typical q values of about 0.27. The typical ratio of m_e to m_f (or m_f to m_e) is $10^{0.27} \approx 1.86$. Thus, the typical values of the mass of young stellar population obtained from fitting of m_f fall in the range from $1.86m_e$ to $m_e/1.86 = 0.54m_e$, where m_e is the estimation obtained from the proposed method. Therefore, we can estimate m with a relative error up to a factor of 1.86. Note that for different galaxies a typical value of m can vary within wide limits and differs by 3 orders of magnitude.

Table 2 Values of q from Eq. 12 for different subsamples derived from luminosities at three wavelength ranges and the oxygen abundance data

Sample	Flux error threshold			
	all (50%)	30%	20%	10%
I.	0.251(207)	0.245(169)	0.210(117)	0.201(45)
II.	0.343(408)	0.344(386)	0.350(344)	0.388(168)
III.	0.305(329)	0.303(311)	0.305(275)	0.322(126)
IV.	0.290(218)	0.285(202)	0.289(175)	0.300(77)
V.	0.315(615)	0.318(555)	0.321(461)	0.358(213)
VI.	0.285(536)	0.284(480)	0.280(392)	0.295(171)
VII.	0.271(425)	0.267(371)	0.260(292)	0.267(122)

NOTE. The number of galaxies is shown in brackets.

In Fig. 2 we show the distribution of the logarithm of the ratio m_e to m_f for the whole sample (sample V). We plot the stacked bar chart for the galaxies with a single star-forming region (subsample VI, grey-shaded histogram) and for the galaxies with several star-forming regions (galaxies entering in the subsample V and missed the subsample VI, black-shaded histogram). One can see that the proposed technique provides better estimation for the galaxies with a single star-forming regions and it should not be applied to galaxies with several obvious knots of star formation.

To estimate the errors in estimation of T_e values we consider T_e and T_f for the subsample VII containing 425 galaxies. We know T_f for each galaxy, as well as either the value of T_e if $T_e > T_0$ or an upper limit T_0 otherwise. The latter circumstance puts some limitations in the direct comparison of T_e and T_f values. We can directly compare T_e and T_f only for 178 galaxies with $T_e > T_0$ and $T_f > T_0$. The mean-root-square value of the difference is 0.87 Myr. For 95 galaxies with $T_e \leq T_0$ and $T_f \leq T_0$ we can only acknowledge a matching of the conclusions from SED fitting and our estimation. For 68 galaxies with $T_e \leq T_0$ and $T_f > T_0$ we for convenience could assign the value $T_e = T_0 = 3.2$ Myr. This keeps the time intervals between starburst age T_f and the upper end of the possible interval $0 < T_e \leq T_0$. The mean-root-square value of the difference $T_f - T_e$ in this case is equal to 0.91 Myr. It is quite reasonable to consider the remaining 84 galaxies with $T_e > T_0$ and $T_f \leq T_0$ in the same way, namely assign the value $T_f = T_0 = 3.2$ Myr instead of the value from SED fitting. The mean-root-square value of the difference $T_f - T_e$ in this case is equal to 1.3 Myr.

In Fig. 3 a histogram of the difference between the estimated T_e and fitted T_f is shown for the entire subsample VII. Here we substituted $T_e = T_0$ if $T_e \leq T_0$ and/or $T_f = T_0$ if $T_f \leq T_0$. A typical value of the difference $T_f - T_e$ is less than 1 Myr. Its overall mean-

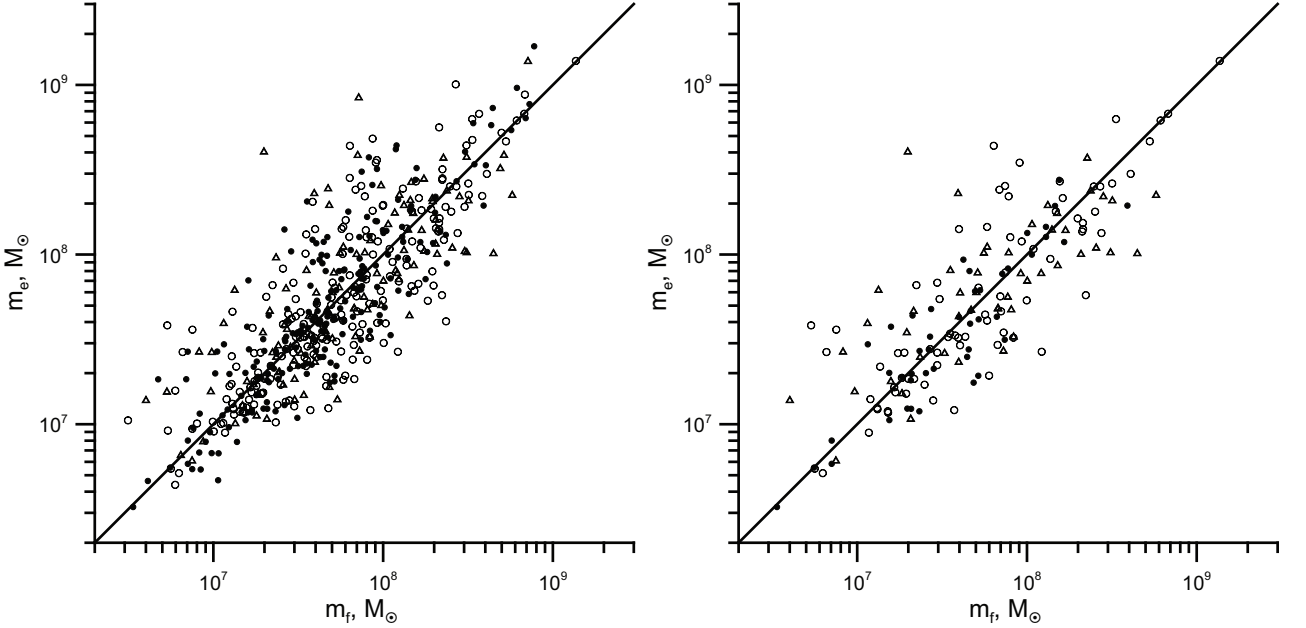


Fig. 1 Comparison of the masses m_e of young stellar population derived from the estimation proposed in Section 3 and masses m_f derived from the SED fitting by Izotov et al. (2011). Dots, open circles and triangles correspond to subsamples of galaxies with “regular”, “irregular” symmetric and “irregular” asymmetric shape. Left panel shows all galaxies from subsample VI, right panel shows only the galaxies with flux errors in UV ranges less than 10%. Solid line corresponds to the equal values

root-square value is 0.87 Myr. There is no systematic shift of the starburst age, as one can see in Fig. 3.

In Fig. 4 we plot T_e vs. T_f for the whole sample. Their comparison makes sense only if both T_e and T_f are greater than $T_0 = 3.2$ Myr. In the Figure, 235 galaxies with a single star-forming region (subsample VI) are shown by dots. We discard one outlier from this subsample. Thirty galaxies with several star-forming regions are shown by crosses. The solid line is the line of equal ages.

We divide the rest of the plot area into three zones A, B and C. Zone A, corresponding to $T_e \leq T_0$, $T_f \leq T_0$, contains 107 galaxies with a single star-forming region and 14 galaxies with several star-forming regions. We assume that T_e and T_f match each other in this case. Zone B corresponds to the case with $T_e \leq T_0$, $T_f > T_0$. The estimations only indicate that $T_e \leq T_0$, therefore the direct comparison is not possible. In Fig. 5 we show the T_f distribution for zones A and B. The left bin corresponds to the zone A with $T_f \leq T_0$. Grey and black regions correspond to the galaxies with a single star-forming region (subsample VI) and to the galaxies with several star-forming regions, respectively.

Zone C corresponds to the case with $T_f \leq T_0$, $T_e > T_0$. In Fig. 6 we show the T_e distribution for zones A and C. The left bin corresponds to the zone A with $T_e \leq T_0$. One can see that the mean difference between T_e and T_f is greater for galaxies with several star-forming

regions. All estimations with $T_e \geq 7.1$ Myr refer to these galaxies only.

Considering the alternative version of the method, described in Section 4, we obtain very poor results. The values of \tilde{T}_e are overestimated. Moreover, numerical solutions of Eqs. 7 and 10 can be obtained only for a part of the sample. If the data scatter were small, both methods would give similar estimations. However, the situation changes in the case of significant scattering. Using the same set of the coefficients in Eq. 5 and 9, we obtain $\tilde{U} = U/m^2$. The set of parameters from Table 1 minimizes U , but we reach the minimum of \tilde{U} at another values of parameters with greater value of \tilde{m}_e . The values of SFR_i fix the combination of parameters in Eq. 2. Thus, the increase of m leads to the decrease of $\tilde{A}f(t) + \tilde{B}\Delta$, i.e. the decrease of $\tilde{f}(t)$ and the increase of t and $\tilde{T}_e = T_0 + t$. However, the approximation Eq. 2 cannot be applied to large starburst ages, when the combination $\tilde{A}f(t) + \tilde{B}\Delta$ changes its sign for LCGs with $\Delta > 0$. As a result, Eqs. 6 and 7 have a discontinuity of the second kind and therefore it is not possible to find any numerical solution for many LCGs. For this reason hereafter we will use only the method described in Section 3.

Note that the small difference in statistical weights between Eqs. 5 and 9 results in an appreciable difference in their application. Thus, hereafter we will use only the first method based on minimization of Eq. 5.

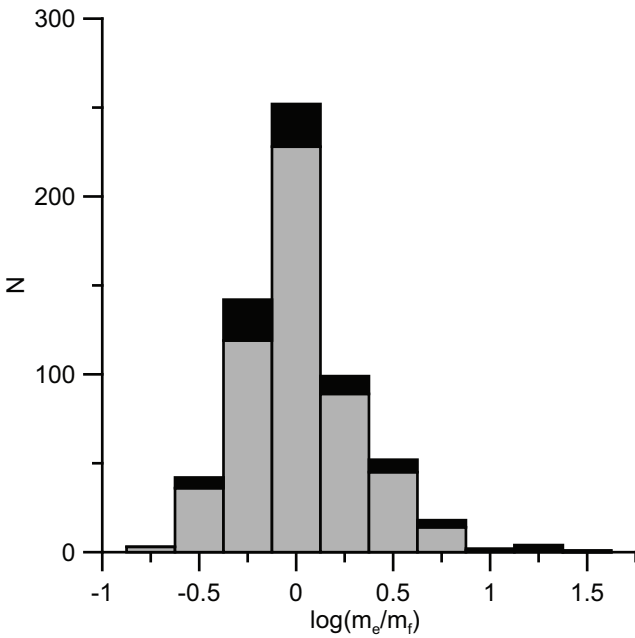


Fig. 2 The distribution of the logarithm of the ratio m_e of young stellar population derived from the estimation proposed in Section 3 to masses m_f derived from the SED fitting by Izotov et al. (2011) for the whole sample. Grey-shaded histogram corresponds to the galaxies with a single star-forming region (subsample VI) and black-shaded histogram corresponds to the galaxies with obvious several star-forming regions. The whole bar (grey plus black) corresponds to the whole sample

8 The estimation of m and T values from the luminosities at three wavelengths without invoking the galaxy oxygen abundances

In order to calculate m_e and T_e one has to know the galaxy H α , FUV and NUV luminosities and the oxygen abundances. However, sometimes the accurate values of the oxygen abundances are not known. We find that using of the mean oxygen abundance $[O]_0$ instead of $[O]_i$ does not lead to the worse accuracy of the m_e and T_e estimation. An algorithm of such estimation differs from the one described in Section 3 by only one detail. Instead of Eq. 2 we use the version with $B = 0$ and substitute this value as B_i in Eqs. 6 and 7. Then we obtain the remaining parameters, namely $p_i = (0.70, 0.28, 0.19)$ and $A_i = (1.98 \times 10^{-7}, 0.70 \times 10^{-7}, 3.16 \times 10^{-7})$ for the subsample VII with UV flux errors less than 20%. These approximations with $B_i = 0$ have the mean errors $\sigma_i = (3.0, 4.2, 4.7)$ and are less accurate than the ones described in Section 6. Nevertheless, with using these approximations we can estimate m and T with errors not exceeding the ones derived with taking into account oxygen abundances for individual objects.

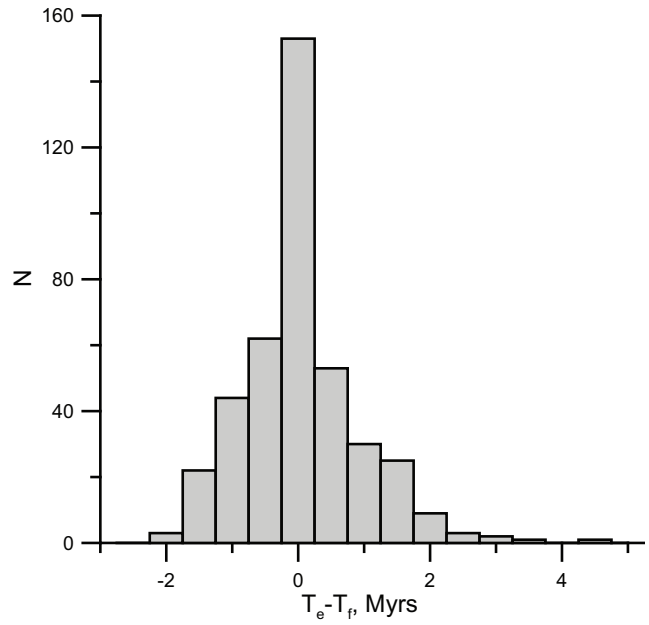


Fig. 3 The distribution of the difference between the star-burst ages T_e estimated from the proposed method and T_f derived from the SED fitting by Izotov et al. (2011) for the subsample VII

We find that the typical value $q \approx 0.28$ (Eq. 13) for the estimation without knowledge of $[O]$ values is the same as that with taking into account the oxygen abundance. The difference $T_e - T_f$ is not changed as well. The mean-root-square values of these differences for the subsamples VI and VII are 0.86 Myr and 0.82 Myr, respectively.

On the other hand, we note that discarding the galaxy metallicities from the parameter set increases the scatter of the approximated SFRs which are derived from H α line and UV luminosities, resulting in higher σ_i as compared to the case considered in Section 6. Therefore, we prefer the approximation which takes into account accurate oxygen abundances for individual galaxies, despite the fact that it does not improve appreciably the determination of m and T .

We note that the analysis in this Section is done for a sample of low-metallicity dwarf galaxies with $[O] = 7.52 - 8.47$, presently experiencing strong bursts of star formation. It may not be applicable for higher-metallicity giant galaxies and/or galaxies with low and modest star formation.

9 The estimation of m and T values from the luminosities at two wavelengths

We consider now the accuracy of the m and T estimation if only H α and FUV luminosities are used. From

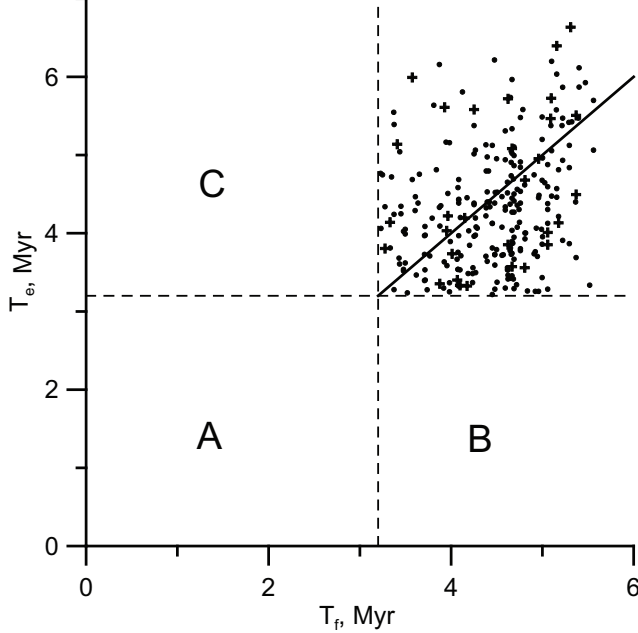


Fig. 4 Comparison of the starburst ages T_e derived from the estimation proposed in Section 3 and T_f derived from the SED fitting by Izotov et al. (2011). Dots and crosses correspond to galaxies with a single star-forming region and with obvious several star-forming regions, respectively. Solid line is the line of equal ages

Eq. 2 we obtain two relations for SFR_1 and SFR_2 , containing two unknown parameters m and T . The values of A_i, B_i and p_i are the ones obtained in Section 6. Assuming $T > T_0$, i.e. $t > 0$, we obtain the equation

$$\begin{aligned} SFR_1 (A_2 \exp(-p_2 t) + B_2 \Delta) = \\ SFR_2 (A_1 \exp(-p_1 t) + B_1 \Delta). \end{aligned} \quad (13)$$

By solving it numerically we obtain the value of t . For $t > 0$ we have an estimation of $T_e = T_0 + t$ and additionally the value of m from Eq. 11. In this case $m_1 = m_2 = m_e$. The values of m_1 and m_2 are equal because of the condition in Eq. 13. For $T < 3.2$ Myr, corresponding to $t < 0$, we adopt $f_i = 1$ and obtain two different estimations of m_1 and m_2 from Eq. 11. We choose a weighted average

$$m_e = \frac{m_1 \sigma_1^{-2} + m_2 \sigma_2^{-2}}{\sigma_1^{-2} + \sigma_2^{-2}} \quad (14)$$

as the estimated value of m_e .

We estimate the values of m and T for galaxies from their H α and FUV luminosities and oxygen abundance for the subsample VII by solving Eq. 13 numerically for 423 galaxies out of 425. The mean difference between the values of m from the estimation and the fitting is characterized by the value $q = 0.55$. Therefore, their

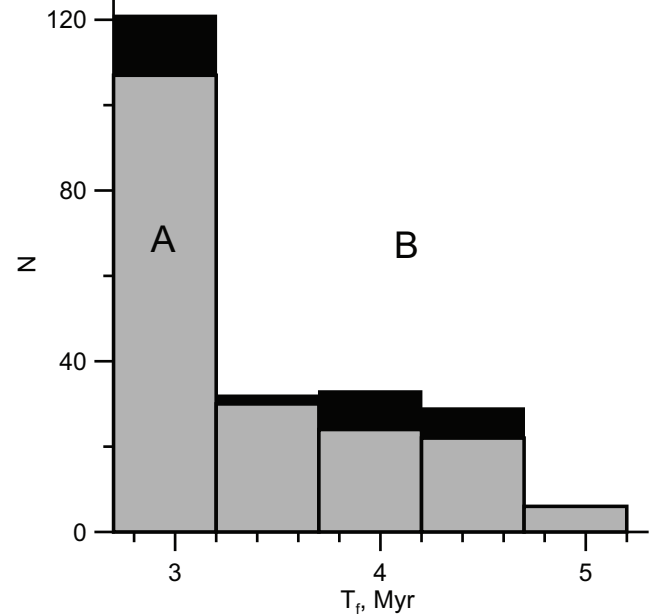


Fig. 5 The T_f distribution in the case $T_e \leq T_0$ (corresponding to zones A and B in Fig. 4). Grey-shaded histogram corresponds to the subsample VI of galaxies with a single star-forming region and black-shaded histogram to the galaxies with several star-forming regions. The whole bar (grey plus black) corresponds to the whole sample

typical ratio is about $10^{0.55} \approx 3.55$. The mean difference between the values of T from the estimation and from the fitting is 1.1 Myr and it drops to 0.9 Myr for the subsample with the errors in FUV fluxes lower than 10%. As expected, the estimations based on two wavelength bands are less accurate than the ones based on three wavelength bands.

Estimating the values of m_e and T_e from the H α line and NUV luminosities we obtain the mean value of q equal to 0.5 and the mean difference of starburst ages equal to 0.83 Myr. This estimation is more accurate compared to the one from the H α line and FUV luminosities due to a larger difference in the values of p_i .

Finally, estimating the values of m_e and T_e from their FUV and NUV luminosities we derive the mean value of q equal to 0.57 and mean difference of starburst ages equal to 1.8 Myr. However, in this case we cannot calculate the estimated values for about 10% galaxies of the sample due to the lack of the data in FUV and/or NUV bands.

10 Summary

We propose a new method for estimation of the mass m and the age T of the young stellar population in Luminous Compact Galaxies (LCGs) from their H α emission

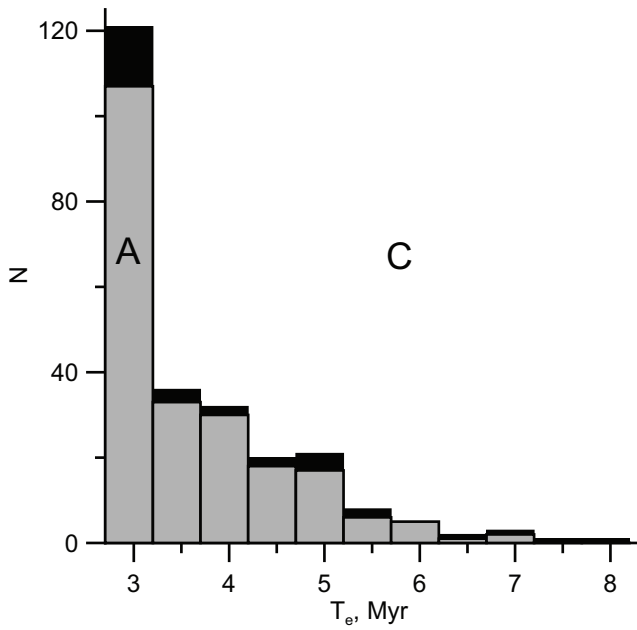


Fig. 6 The T_e distribution in the case $T_f \leq T_0$ (corresponding to zones A and C in Fig. 4). Grey-shaded histogram corresponds to the subsample VI of galaxies with a single star-forming region and black-shaded histogram to the galaxies with several star-forming regions. The whole bar (grey plus black) corresponds to the whole sample

line, *GALEX* far-UV (FUV) and near-UV (NUV) continuum luminosities as well as their oxygen abundances. No time-consuming fitting of spectral energy distribution (SED) is needed for this purpose.

This method was validated on the sample of about 800 LCGs constructed by Izotov et al. (2011) and used by Parnovsky et al. (2013). The typical deviations of m and T values derived with technique proposed in this paper from those obtained by Izotov et al. (2011) from the SED fitting is 0.27 for $\log m$ and 0.87 Myr for T .

The proposed method provides fairly accurate estimations for galaxies with a single star-forming region and is slightly more accurate for galaxies without evident asymmetry. It fails to reproduce fitted m and T for galaxies with several distinguishable knots of star formation.

Adopting k of 7.9×10^{-42} for the $\text{H}\alpha$ luminosity and of 1.4×10^{-28} for the FUV and NUV ranges, we recommend the following values of the parameters to use in the determination of m and T : $\sigma_i = (3.0, 4.2, 4.7)$, $p_i = (0.72, 0.35, 0.27)$, $A_i = (2.06 \times 10^{-7}, 1.04 \times 10^{-7}, 1.43 \times 10^{-7})$ and $B_i = (-4.72 \times 10^{-8}, -6.21 \times 10^{-8}, -9.21 \times 10^{-8})$.

We find that for galaxies with low metallicities one can use the mean $[\text{O}]$ value instead of individual one without worsening the accuracy of the m and T estimation.

We also considered the estimation of m and T from the luminosities at two wavelengths. It is less accurate, especially for estimation of m . The typical error of $\log m$ is more than 0.5 in this case.

The proposed method can be used for preparing the samples of galaxies with the desired ranges of discussed parameters, preliminary selection of galaxies entering some samples or for reducing of a range of parameter variations for SED fitting.

We thank the anonymous referee for valuable comments which helped to improve the presentation of results.

GALEX is a NASA Small Explorer launched in April 2003. We gratefully acknowledge NASA's support for construction, operation and science analysis for *GALEX* mission, developed in cooperation with the Centre National d'Etudes Spatiales of France and the Korean Ministry of Science and Technology.

Funding for the Sloan Digital Sky Survey (SDSS) and SDSS-II has been provided by the Alfred P. Sloan Foundation, the Participating Institutions, the National Science Foundation, the U.S. Department of Energy, the National Aeronautics and Space Administration, the Japanese Monbukagakusho, and the Max Planck Society, and the Higher Education Funding Council for England.

Table 1 Values of the coefficients in Eqs. 2 and 3 for different subsamples of LCGs

Err	H α				FUV				NUV							
	<i>N</i>	σ_1	p_1	$A_1 \times 10^7$	$B_1 \times 10^8$	<i>N</i>	σ_2	p_2	$A_2 \times 10^7$	$B_2 \times 10^8$	<i>N</i>	σ_3	p_3	$A_3 \times 10^7$	$B_3 \times 10^8$	
I. “Regular”																
all	276	3.3	0.67	1.92 \pm 0.03	-4.4 \pm 1.0	212	4.4	0.39	1.33 \pm 0.04	-5.6 \pm 1.4	232	5.1	0.31	1.58 \pm 0.04	-5.1 \pm 1.5	
30%	172	3.4	0.72	1.97 \pm 0.04	-5.0 \pm 1.2	169	4.4	0.39	1.36 \pm 0.04	-7.4 \pm 1.5	169	4.9	0.32	1.61 \pm 0.04	-4.8 \pm 1.7	
20%	120	3.1	0.70	1.98 \pm 0.05	-3.1 \pm 1.2	117	3.7	0.21	0.98 \pm 0.03	-9.2 \pm 1.5	117	3.6	0.13	1.14 \pm 0.03	-5.1 \pm 1.7	
10%	47	2.5	0.73	2.32 \pm 0.09	-7.4 \pm 2.5	45	2.3	0.47	1.18 \pm 0.07	-12.6 \pm 2.4	45	2.2	0.30	1.32 \pm 0.06	-10.7 \pm 2.4	
II. “Irregular”																
all	519	3.6	0.64	1.82 \pm 0.02	-3.3 \pm 0.6	418	4.4	0.40	0.98 \pm 0.02	-3.9 \pm 0.9	435	7.3	0.33	1.64 \pm 0.03	-12.6 \pm 1.5	
30%	391	3.3	0.67	1.90 \pm 0.02	-3.8 \pm 0.7	388	4.4	0.41	1.00 \pm 0.02	-3.6 \pm 0.9	387	6.3	0.33	1.60 \pm 0.03	-11.9 \pm 1.3	
20%	348	3.3	0.66	1.90 \pm 0.03	-5.7 \pm 0.9	346	4.3	0.41	1.03 \pm 0.03	-6.4 \pm 1.2	345	6.0	0.34	1.59 \pm 0.04	-13.1 \pm 1.7	
10%	171	3.5	0.64	1.80 \pm 0.04	-5.1 \pm 1.2	170	4.7	0.42	1.01 \pm 0.04	-4.9 \pm 1.6	169	6.3	0.34	1.61 \pm 0.04	-14.8 \pm 2.1	
III. “Irregular” with a single star-forming region																
all	415	3.4	0.65	1.85 \pm 0.02	-2.6 \pm 0.7	333	3.8	0.48	1.07 \pm 0.03	-2.2 \pm 0.9	351	7.2	0.39	1.79 \pm 0.04	-13.9 \pm 1.6	
30%	312	2.8	0.73	2.07 \pm 0.03	-4.0 \pm 0.7	312	3.7	0.48	1.07 \pm 0.03	-2.3 \pm 0.9	312	6.1	0.37	1.69 \pm 0.04	-12.9 \pm 1.4	
20%	276	2.8	0.73	2.11 \pm 0.03	-5.9 \pm 0.9	276	3.7	0.48	1.09 \pm 0.03	-4.8 \pm 1.2	276	6.0	0.40	1.70 \pm 0.04	-15.5 \pm 1.8	
10%	127	2.2	0.74	2.11 \pm 0.03	-5.4 \pm 0.9	127	3.7	0.51	1.11 \pm 0.04	-3.3 \pm 1.5	127	5.3	0.42	1.77 \pm 0.05	-19.7 \pm 2.1	
IV. “Irregular” with a single star-forming region without asymmetry																
all	275	3.5	0.70	2.01 \pm 0.03	-4.2 \pm 0.9	219	3.9	0.42	1.01 \pm 0.04	-0.3 \pm 1.0	232	7.2	0.36	1.72 \pm 0.05	-14.3 \pm 1.9	
30%	202	2.9	0.73	2.06 \pm 0.03	-3.6 \pm 0.8	202	3.9	0.41	1.00 \pm 0.03	-0.3 \pm 1.1	202	5.3	0.33	1.58 \pm 0.03	-13.3 \pm 1.4	
20%	175	2.9	0.74	2.13 \pm 0.03	-6.3 \pm 1.1	175	3.9	0.42	1.03 \pm 0.03	-2.7 \pm 1.4	175	5.2	0.33	1.57 \pm 0.04	-15.7 \pm 1.9	
10%	77	1.7	0.74	2.12 \pm 0.03	-5.0 \pm 0.9	77	3.8	0.50	1.13 \pm 0.09	1.9 \pm 2.1	77	5.2	0.41	1.85 \pm 0.06	-14.0 \pm 4.3	
V=I+II. All																
all	795	3.5	0.65	1.85 \pm 0.02	-3.6 \pm 0.5	630	4.6	0.43	1.12 \pm 0.02	-5.1 \pm 0.8	667	6.7	0.33	1.63 \pm 0.03	-10.2 \pm 1.1	
30%	563	3.3	0.68	1.91 \pm 0.02	-4.1 \pm 0.6	557	4.7	0.43	1.14 \pm 0.02	-5.2 \pm 0.8	556	6.0	0.33	1.60 \pm 0.02	-10.0 \pm 1.1	
20%	468	3.3	0.67	1.91 \pm 0.02	-4.8 \pm 0.7	463	4.4	0.35	1.03 \pm 0.02	-8.3 \pm 1.0	462	5.6	0.30	1.49 \pm 0.03	-10.8 \pm 1.2	
10%	218	3.4	0.66	1.87 \pm 0.03	-5.8 \pm 1.1	215	4.3	0.43	1.04 \pm 0.03	-5.7 \pm 1.4	214	5.7	0.33	1.57 \pm 0.04	-14.2 \pm 1.8	
VI=I+III. All with a single star-forming region																
all	691	3.4	0.66	1.88 \pm 0.02	-3.2 \pm 0.5	545	4.3	0.47	1.20 \pm 0.02	-3.9 \pm 0.8	583	6.5	0.37	1.72 \pm 0.03	-10.8 \pm 1.2	
30%	484	3.0	0.72	2.02 \pm 0.02	-4.2 \pm 0.6	481	4.4	0.46	1.19 \pm 0.02	-4.3 \pm 0.8	481	5.7	0.36	1.67 \pm 0.03	-10.5 \pm 1.1	
20%	396	2.9	0.72	2.06 \pm 0.02	-4.8 \pm 0.7	393	4.0	0.39	1.07 \pm 0.02	-7.7 \pm 1.0	393	5.3	0.34	1.55 \pm 0.03	-12.1 \pm 1.3	
10%	173	2.3	0.75	2.16 \pm 0.03	-5.7 \pm 0.9	172	3.5	0.51	1.15 \pm 0.03	-4.5 \pm 1.3	172	4.8	0.39	1.67 \pm 0.04	-18.3 \pm 1.8	
VII=I+IV. All with a single star-forming region without asymmetry																
all	551	3.4	0.69	1.98 \pm 0.02	-4.4 \pm 0.7	431	4.5	0.43	1.18 \pm 0.02	-2.3 \pm 0.9	464	6.3	0.33	1.64 \pm 0.03	-10.0 \pm 1.2	
30%	374	3.1	0.73	2.03 \pm 0.03	-4.2 \pm 0.7	371	4.6	0.43	1.19 \pm 0.03	-2.7 \pm 1.0	371	5.2	0.33	1.61 \pm 0.03	-9.9 \pm 1.1	
20%	295	3.0	0.72	2.06 \pm 0.03	-4.7 \pm 0.8	292	4.2	0.35	1.04 \pm 0.02	-6.2 \pm 1.1	292	4.7	0.27	1.43 \pm 0.02	-9.2 \pm 1.3	
10%	124	2.1	0.76	2.22 \pm 0.03	-5.4 \pm 1.0	122	3.5	0.52	1.24 \pm 0.04	-1.5 \pm 1.7	122	4.5	0.36	1.67 \pm 0.04	-13.6 \pm 2.1	

NOTE. The values of p_i are in Myr^{-1} , standard deviations σ_i are in $M_\odot \text{ yr}^{-1}$, coefficients A_i and B_i in Eq. 2 are in yr^{-1} , N is the number of the galaxies in the subsample. The “Err” column indicates the threshold of the measured UV flux errors, the label “all” corresponds to the 50% level.

References

Abazajian, K. N., Adelman-McCarthy, J. K., Agueros, M. A., et al. 2009, *Astrophys. J. Suppl. Ser.*, 182, 543

Amorín, R. O., Pérez-Montero, E., & Vilchez, J. M. 2010, *Astrophys. J.*, 715, L128

Calzetti, D. 2012, preprint arXiv:1208.2997v1

Cardamone, C., Schawinski, K., Sarzi, M., et al. 2009, *Mon. Not. R. Astron. Soc.*, 399, 1191

Cardelli, J.A., Clayton, G. C., & Mathis J. S. 1989, *Astrophys. J.*, 345, 245

Fisher, R. A. 1954, “Statistical methods for research workers”, Oliver and Boyd: London

Hawley, S. A. 2012, *Publ. Astron. Soc. Pac.*, 124, 21

Hudson, D. J. 1964, “Statistics Lectures on Elementary Statistics and Probability”, CERN: Geneva

Izotov, Y. I., Guseva, N. G., & Thuan, T. X. 2011, *Astrophys. J.*, 728, 161

Kennicutt, R. C., Jr. 1998, *Annu. Rev. Astron. Astrophys.*, 36, 189

Parnovsky, S.L., Izotova I.Yu., & Izotov Y.I. 2013, *Astrophys. Space Sci.*, 343, 361

Pilyugin, L.S., Vilchez, J.M., Mattsson, L., & Thuan, T. X. 2012, *Mon. Not. R. Astron. Soc.*, 421, 1624

Salpeter, E.E. 1955, *Astrophys. J.*, 121, 161